

SUPERCONDUCTING MULTICELL CAVITY WITH REENTRANT CELLS

Valery Shemelin, Hasan Padamsee

Laboratory for Elementary-Particle Physics, Cornell University, Ithaca, NY 14853

INTRODUCTION

The successful test of the first one-cell reentrant cavity [1] showed that technological challenges inherent to this shape can be overcome. Now we need to further confirm this approach and test a multicell reentrant cavity. In this paper it is not proposed to solve the problems with propagation of higher order modes, we will concentrate on the geometrical solution for optimization of peak field, so the diameters of beam pipes and iris apertures are chosen both equal to 70 mm. The proposed geometry is as simple as possible for the reentrant case. Each half-cell consists of two elliptic arcs. Geometry and designation of dimensions are shown in Fig. 1.

DIMENSIONS OF CELLS

As it was done for the one-cell reentrant cavity, we will choose the version with 20 % higher electric field and 10 % lower magnetic field in comparison to the TESLA inner cells. Let us keep the geometry of the inner half of the end cells the same as of the inner cells. Optimization of the end half-cell can be done in the same manner as it was done for inner cells [2] but now we have fixed equatorial radius. Tuning to the correct frequency for the end half-cell (or the end cup) can be done by changing the length of this cup (L_e). For optimization, 3 half-axes were varied (A , B , and a). Half-axis b is defined by geometrical restrictions: by length L and equatorial radius R_{eq} . The obtained shape of the end cell is shown in Fig. 2, the dimensions – half-axes of conjugated ellipses, radii and lengths are presented in Table 1. An inner cell consists of two (one of them is mirror-reflected) left half-cells from Fig. 2.

Table 1. Dimensions of the inner and end cell, mm

	Inner cup (subscript i in Fig.1)	End cup (subscript e in Fig.1)
A	51.56	53.53
B	36.22	42.79
a	9.16	4.59
b	11.92	7.743
L	57.652	56.238
R_{bp}	35	
R_{eq}	98.710	

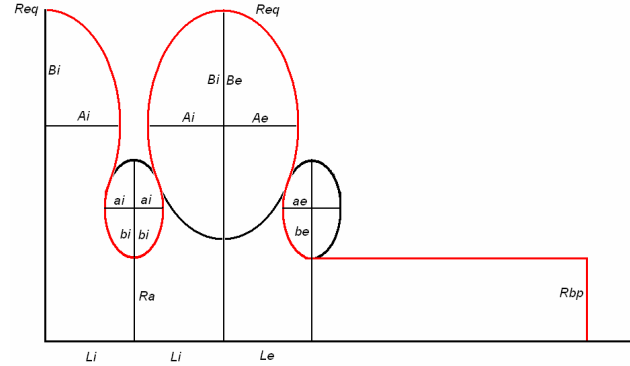


Fig. 1. Geometry and designation of dimensions for the inner and end cells.

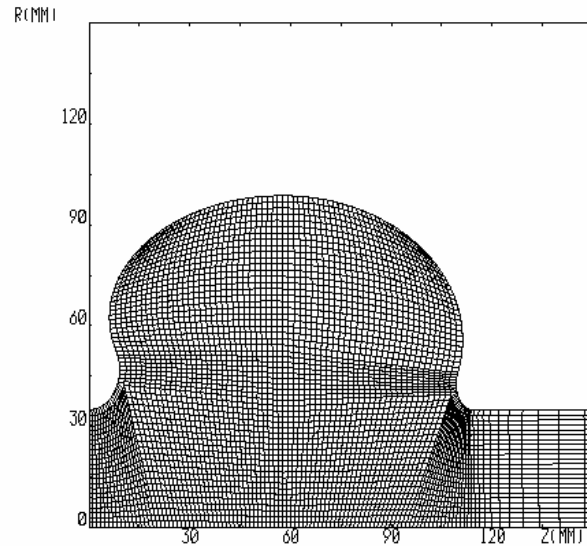


Fig. 2. Optimized shape of the end cell (SLANS mesh is shown).

The calculated values of peak electric and magnetic fields normalized to acceleration in the cell are as follows: for the inner cell $E_{pk}/E_{acc} = 2.40$ (+20 % to TESLA), $H_{pk}/E_{acc} = 37.8$ Oe/(MV/m) (-10 % to TESLA), for the end cell $E_{pk}/E_{acc} = 2.39$, $H_{pk}/E_{acc} = 37.6$ Oe/(MV/m). R/Q and G parameters for the inner cells are 120.6 Ohm and 280 Ohm, and for the end cells, 120.9 and 286 Ohm, respectively.

One can see that values of E_{pk}/E_{acc} and H_{pk}/E_{acc} are a little bit smaller for the end cell. This means that E_{acc} is slightly bigger because peak fields are the same in both inner and end cell. This difference is negligible (acceleration of the last cell is about 0.4 % higher than of the inner one); however, without optimization of the end cell this cell can have lower acceleration. For example, our calculations show that TESLA end cells (Fig. 5) have 1.3 % and 1.1 % lower acceleration than inner cells.

REQUIREMENTS TO DIMENSIONS' ACCURACY

Errors of dimensions inevitable by fabrication will change the optimized values of normalized electric and magnetic peak fields and frequency. To find the allowable

departures of dimensions we have to analyze dependences of normalized peak fields and frequency on the cavity dimensions. Dependences for inner cells are presented in Fig. 3, for the end cells – in Fig. 4. Here for normalization we used parameters $e = E_{pk}/2E_{acc}$, and $h = H_{pk}/42E_{acc}$. This normalization is made for easier comparison to TESLA inner cells [3], because these cells have $E_{pk}/E_{acc} = 2.0$ and $H_{pk}/E_{acc} = 42 \text{ Oe}/(\text{MV}/\text{m})$, so that for them $e = 1$ and $h = 1$. The results taken from these graphs are presented in Table 2. As can be seen from the Table, most important are tolerances of the big half-axis A : to keep the value of e with precision 0.01 we need to make the A for the end cup with error not more than +0.14 mm (Fig. 4, upper left picture). The negative error

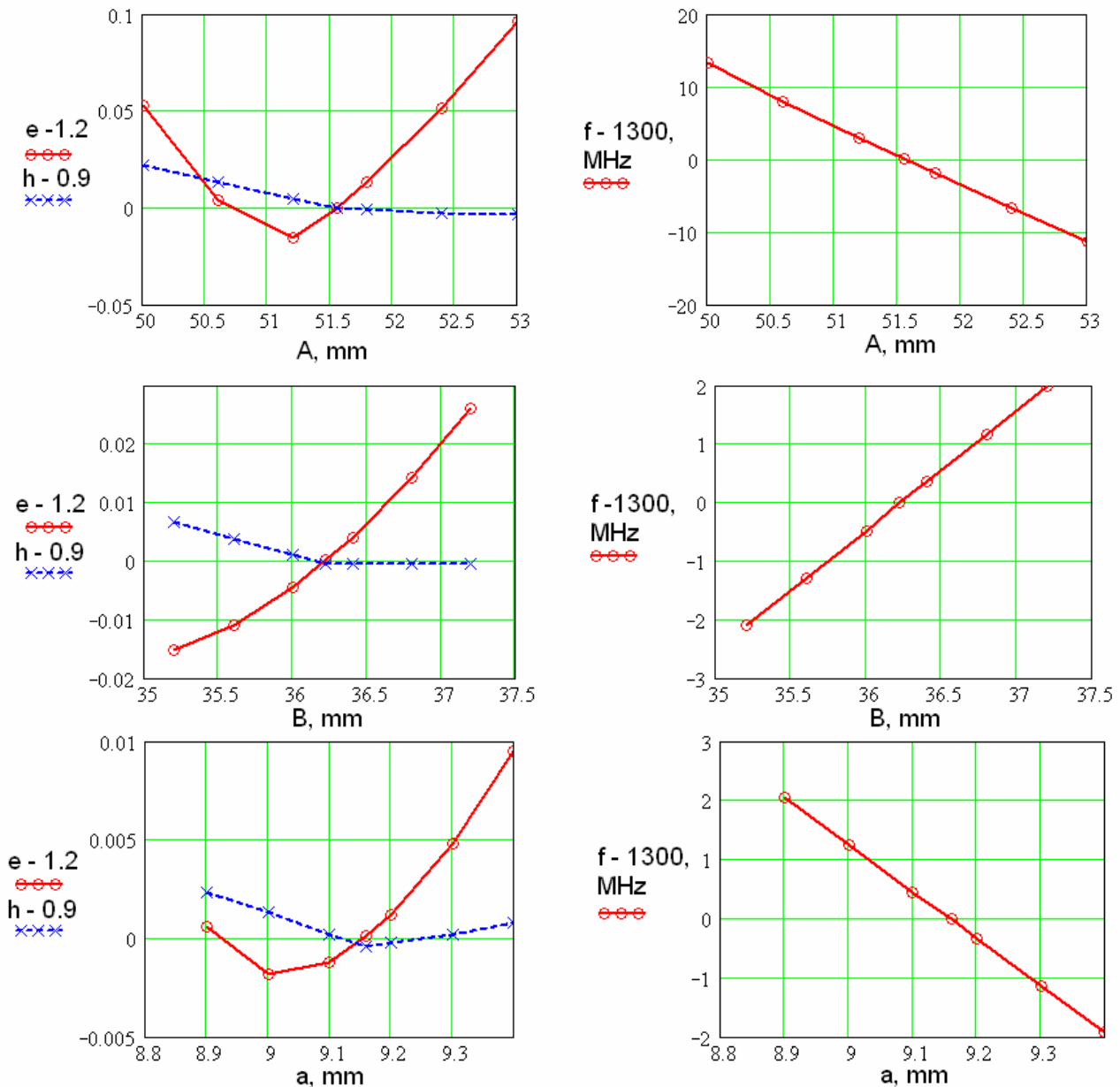


Fig. 3. Change of e , h and f by not exact execution of dimensions of the inner cell.

Table 2. Derivatives of parameters e and h , and frequency f with respect to dimensions of the inner and end cells.

		$\frac{\partial e}{\partial A}$, mm ⁻¹	$\frac{\partial e}{\partial B}$, mm ⁻¹	$\frac{\partial e}{\partial a}$, mm ⁻¹	$\frac{\partial h}{\partial A}$, mm ⁻¹	$\frac{\partial h}{\partial B}$, mm ⁻¹	$\frac{\partial h}{\partial a}$, mm ⁻¹	$\frac{\partial f}{\partial A}$, MHz/mm	$\frac{\partial f}{\partial B}$, MHz/mm	$\frac{\partial f}{\partial a}$, MHz/mm
Inner cell		0.054	0.022	0.028	-0.014	-0.007	-0.010	-8.2	2.0	-8.0
End cell	Inner cup	0.060	0.016	0.032	0.006	-0.007	0.012	-4.1	1.0	-4.0
	End cup	0.073	0.018	0.032	-0.013	0.003	-0.007	-3.4	1.2	-2.4
		$\frac{\partial e}{\partial R_{eq}}$, mm ⁻¹	$\frac{\partial e}{\partial R_a}$, mm ⁻¹	$\frac{\partial e}{\partial L}$, mm ⁻¹	$\frac{\partial h}{\partial R_{eq}}$, mm ⁻¹	$\frac{\partial h}{\partial R_a}$, mm ⁻¹	$\frac{\partial h}{\partial L}$, mm ⁻¹	$\frac{\partial f}{\partial R_{eq}}$, MHz/mm	$\frac{\partial f}{\partial R_a}$, MHz/mm	$\frac{\partial f}{\partial L}$, MHz/mm
Inner cell		-0.018	0.034	-0.052	-0.005	0.010	0.016	-14.7	4.1	7.1
End cell	Inner cup	-0.028	0.026	-0.044	-0.008	0.001	0.005	-14.5	2.1	3.5
	End cup		0.009	-0.070		0.008	0.005		1.2	2.9

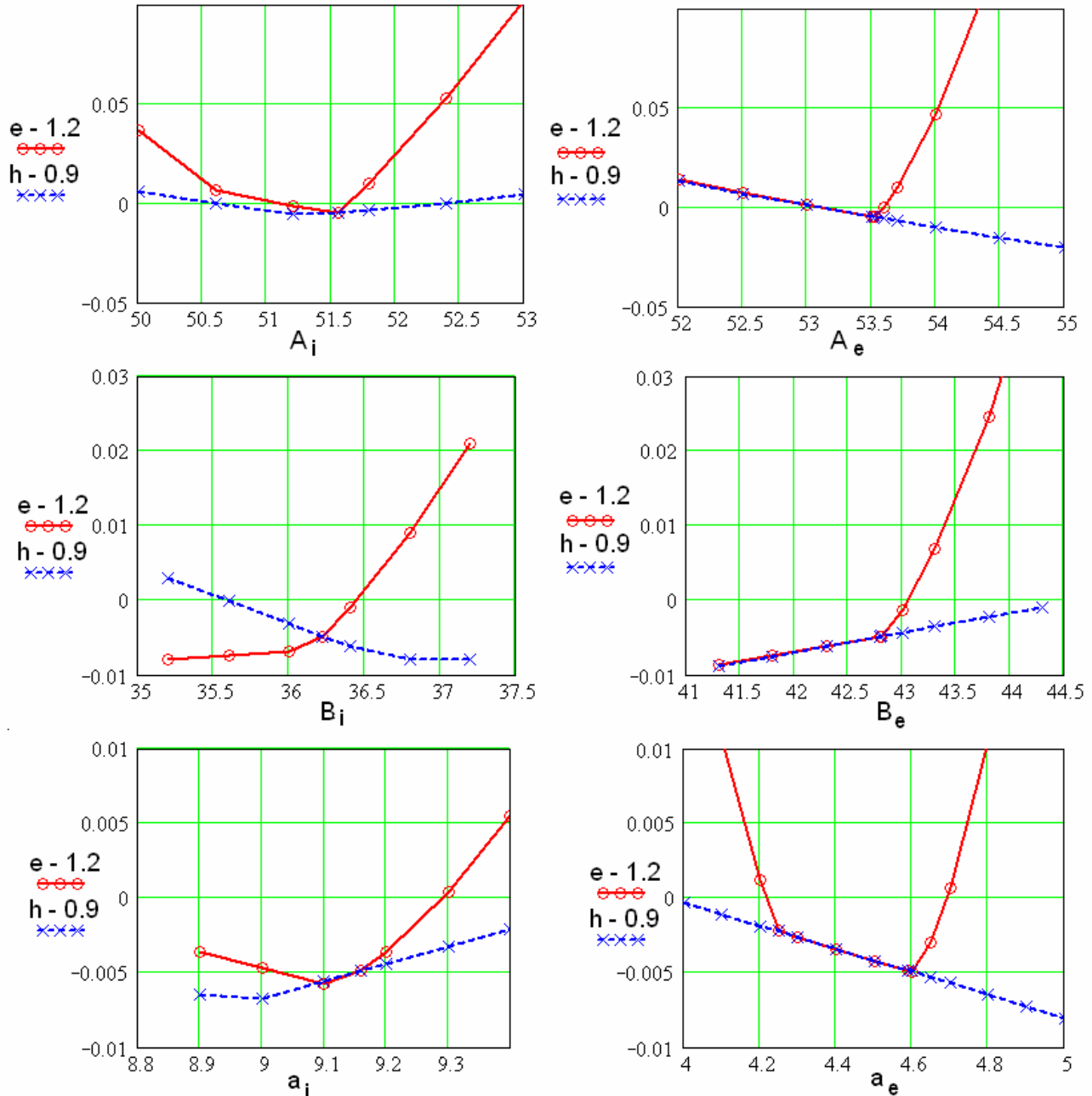


Fig. 4. Change of e and h by not exact execution of dimensions of the end cell, for the inner (left pictures) and for the end cup (right).

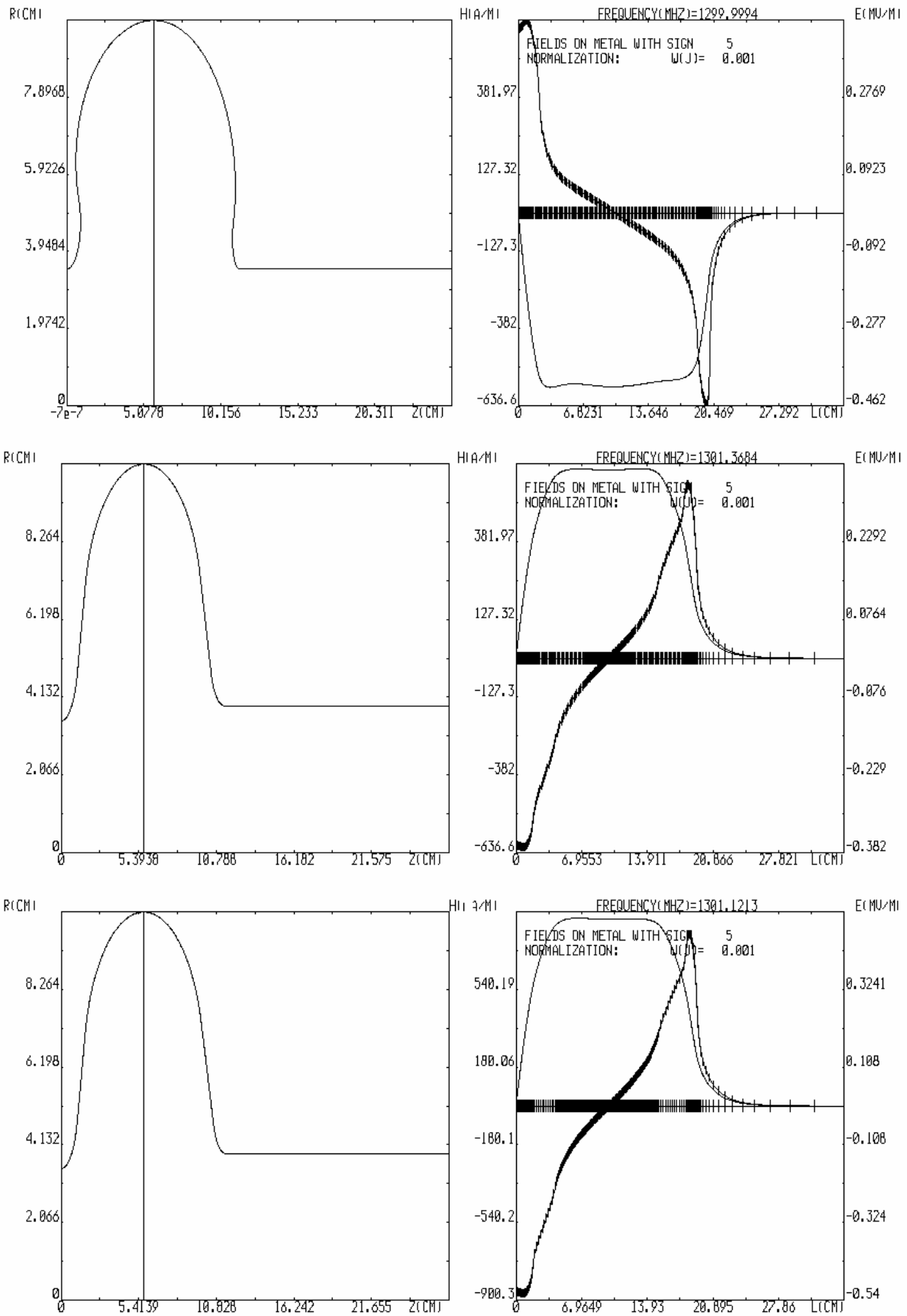


Fig. 5. Profile and fields along the profile line for the optimized reentrant cavity (upper pictures), and for comparison for two different TESLA end cells (TESLA cavity has different end cells [3]).

of this dimension, as can be seen from the graph can be tolerated several times bigger. To keep frequency error within ± 0.1 MHz, the same half-axis should be made with precision ± 12 μm . The step-like change of the value of derivatives for values of e and h is caused by jump-like transition of the location of the peak field from one place to another when one of dimensions changes continuously. Derivatives of frequency with respect to different dimensions are 2 times smaller for the inner half of the end cell than for the inner cell because for the inner cell we changed both sides of the elliptic arc having the same dimension. For the end cell each half was changed separately.

Maximal influence on frequency has the equatorial radius R_{eq} : 14.5 – 14.7 MHz/mm, or 7 μm per 0.1 MHz.

Fortunately, this parameter has a mean influence on e and h . Big influence on e has error of the cup length. Parameters to be executed most accurately are highlighted in Table 2.

Dimensions of the tested reentrant cavity [1] are close to optimal but nevertheless are not exactly optimal. The optimal dimensions for one-cell cavity are dimensions of the end cup of the end cell (Table 1) because both halves of the one-cell cavity are “end cups”. The length of this cavity is about 3 % shorter than half-wave length but it does not matter because physically fields are not limited by this length.

FIELDS ALONG THE PROFILE LINE

Electric and magnetic fields along the profile line of the end cell are shown in Fig. 5. Fields along the profile line of the inner cell can be obtained from the same graph if we symmetrically (mirror symmetry for magnetic, and central symmetry for electric field) reflect the left part of the graph. Maximal acceleration in the last cell is limited by electric field, so maximal electric fields on both sides of the cavity become equal in the process of optimization. This resource was not used, for example, in the TESLA end cells, Fig. 5. However, in the design of TESLA cavity problems with HOM extraction were being solved which are not discussed in the present paper.

REFERENCES

- [1] R. L. Geng, H. Padamsee, A. Seaman, V. D. Shemelin. World Record Accelerating Gradient Achieved in a Superconducting Niobium RF Cavity. PAC 2005, Knoxville, TN, May 2005.
- [2] V. Shemelin, H. Padamsee, R. L. Geng. Optimal Cells for TESLA Accelerating Structure. Nucl. Instr. and Meth. A496, (2003), 1 – 7.
- [3] D. A. Edwards (ed.). TESLA Test Facility Linac – Design Report. DESY Print, March 1995, TESLA 95-01.